



## Research Article

<https://doi.org/10.1631/jzus.B2200503>



# FOXO1-miR-506 axis promotes chemosensitivity to temozolomide and suppresses invasiveness in glioblastoma through a feedback loop of FOXO1/miR-506/ETS1/FOXO1

Chao CHEN<sup>1\*</sup>, Yu'e LIU<sup>2\*</sup>, Hongxiang WANG<sup>1</sup>, Xu ZHANG<sup>1</sup>, Yufeng SHI<sup>2✉</sup>, Juxiang CHEN<sup>1✉</sup>

<sup>1</sup>Department of Neurosurgery, Changhai Hospital, Second Military Medical University, Shanghai 200433, China

<sup>2</sup>Tongji University Cancer Center, Shanghai Tenth People's Hospital of Tongji University, School of Medicine, Tongji University, Shanghai 200092, China

**Abstract:** To explore the role of forkhead box protein O1 (FOXO1) in the progression of glioblastoma multiforme (GBM) and related drug resistance, we deciphered the roles of FOXO1 and miR-506 in proliferation, apoptosis, migration, invasion, autophagy, and temozolomide (TMZ) sensitivity in the U251 cell line using in vitro and in vivo experiments. Cell viability was tested by a cell counting kit-8 (CCK8) kit; migration and invasion were checked by the scratching assay; apoptosis was evaluated by terminal deoxynucleotidyl transferase dUTP nick-end labeling (TUNEL) staining and flow cytometry. The construction of plasmids and dual-luciferase reporter experiment were carried out to find the interaction site between FOXO1 and miR-506. Immunohistochemistry was done to check the protein level in tumors after the in vivo experiment. We found that the FOXO1-miR-506 axis suppresses GBM cell invasion and migration and promotes GBM chemosensitivity to TMZ, which was mediated by autophagy. FOXO1 upregulates miR-506 by binding to its promoter to enhance transcriptional activation. MiR-506 could downregulate E26 transformation-specific 1 (ETS1) expression by targeting its 3'-untranslated region (UTR). Interestingly, ETS1 promoted FOXO1 translocation from the nucleus to the cytosol and further suppressed the FOXO1-miR-506 axis in GBM cells. Consistently, both miR-506 inhibition and ETS1 overexpression could rescue FOXO1 overactivation-mediated TMZ chemosensitivity in mouse models. Our study demonstrated a negative feedback loop of FOXO1/miR-506/ETS1/FOXO1 in GBM in regulating invasiveness and chemosensitivity. Thus, the above axis might be a promising therapeutic target for GBM.

**Key words:** Glioblastoma; Forkhead box protein O1 (FOXO1); MiR-506; E26 transformation specific-1 (ETS1); Chemosensitivity

## 1 Introduction

Glioblastoma multiforme (GBM; World Health Organization (WHO) grade IV glioma) is the most common and lethal malignant brain tumor in adults, with a dismal prognosis despite multimodality treatments, including surgery, radiotherapy, and chemotherapy (Lapointe et al., 2018; Louis et al., 2021). GBM has been characterized by high invasiveness with multiple lesions and dissemination as well as resistance to

radiotherapy and chemotherapy (Phillips et al., 2006). Temozolomide (TMZ) is a first-choice alkylating agent accepted as a gold standard of GBM (Lwin et al., 2013; Tomar et al., 2021). However, most GBM patients present with local recurrence due to TMZ resistance and high invasive capacity (Lwin et al., 2013; de la Rosa et al., 2020). Therefore, understanding the mechanisms of TMZ resistance and high invasiveness is crucial for the discovery of novel targets for GBM treatment.

Forkhead box protein O1 (FOXO1) belongs to the subfamily of forkhead transcription factors. FOXO1 is known to be located at the vital node of a pathway of receptor tyrosine kinases (RTKs), which is closely related to RTK pathway phosphorylation and activity (The Cancer Genome Atlas Research Network, 2008). In our previous study, we found that high cytoplasmic FOXO1 expression was an independent prognostic

✉ Juxiang CHEN, [juxiangchen@126.com](mailto:juxiangchen@126.com)

Yufeng SHI, [yshi@tongji.edu.cn](mailto:yshi@tongji.edu.cn)

\* The two authors contributed equally to this work

✉ Chao CHEN, <https://orcid.org/0000-0001-8173-218X>

Yufeng SHI, <https://orcid.org/0000-0003-3833-1035>

Received Oct. 25, 2022; Revision accepted Mar. 22, 2023;  
Crosschecked June 16, 2023

© Zhejiang University Press 2023

factor for overall survival and progression-free survival in glioblastoma, which indicated that the inactivation of FOXO1 was closely related to the poor prognosis of glioblastoma (Chen et al., 2013). FOXO1 plays a key role in multidrug resistance (MDR) and invasion in glioblastoma (Chen et al., 2019), while the upstream or downstream molecular mechanism has not yet been elucidated.

MicroRNA, a type of non-coding and single-stranded RNA, plays a regulative role in gene expression. The expression profiles of GBM-derived microRNA showed a different pattern between long-term and short-term survivors (Schneider et al., 2023). It was reported that miR-506 was upregulated by FOXO1 in the human embryonic kidney cell lines (Singhal et al., 2013). High expression of miR-506 suppressed the metastasis of colorectal tumor (Wei et al., 2019) and gastric tumor (Wang et al., 2019). However, whether the FOXO1-miR-506 axis involves TMZ resistance and the high invasiveness of GBM remains unclear.

As a member of the E26 transformation-specific (ETS) family, ETS1 is reported to be involved in cell proliferation, survival, and invasion, and associated with poor prognosis and therapy resistance in cancers (Vishnoi et al., 2020). MiR-506 has been demonstrated to inhibit epithelial-mesenchymal transition (EMT) and angiogenesis in gastric cancer by targeting ETS1 (Li et al., 2015).

In this study, we aimed to explore whether a feedback loop of the FOXO1/miR-506/ETS1/FOXO1 exists in association with TMZ sensitivity and tumor invasion in GBM. Our results provide a new idea for the treatment of GBM regarding TMZ resistance.

## 2 Materials and methods

### 2.1 Cell lines and treatments

Human brain tumor cell lines U251, SHG-44, U87, and A172 were purchased from the Cell Bank of the Chinese Academy of Sciences (Shanghai, China). Human astrocytes (HAs) were supplied by ScienCell Research Laboratories (CA, USA). Cells of U251 and A172 were maintained in Dulbecco's modified Eagle's medium (DMEM), SHG-44 in Roswell Park Memorial Institute (RPMI)-1640, and U87 in minimum essential medium (MEM) appended with 10% (0.1 g/mL) fetal bovine serum (FBS). All the above media and FBS

were supplied by GIBCO-Invitrogen (Grand Island, NY, USA). HA was cultured using astrocyte medium (ScienCell). All cell lines were cultured under the conditions of 37 °C and 5% CO<sub>2</sub>. Cells were transfected with FOXO1 overexpression (FOXO1-OE) and negative control (NC) plasmids according to a previous study (Chen et al., 2019). U251 was treated with 0–1500 μmol/L TMZ in 0.5% (volume fraction) dimethyl sulfoxide (DMSO; Sigma, USA, T2577).

### 2.2 Apoptosis assay by TUNEL staining and flow cytometry

The apoptosis assay was conducted using the terminal deoxynucleotidyl transferase dUTP nick-end labeling (TUNEL) staining kit (Roche, Switzerland) and Annexin V-fluorescein isothiocyanate (FITC)/propidium iodide (PI) cell apoptosis detection kit according to the manufacturer's protocol. Briefly, the control cells, plasmids of FOXO1-OE, or control vector (NC) plasmids, or miR-506-3p inhibitor (RiboBio, Guangzhou, China) transfected cells treated with/without a final concentration of 50 μmol/L TMZ in 0.5% DMSO were prepared for TUNEL staining according to the kit instructions. Finally, the TUNEL-positive cells were visualized and imaged with a fluorescence microscope (Leica, Germany).

For detection by flow cytometry, cells were digested with 0.25% (2.5 g/L) trypsin without ethylenediaminetetraacetic acid (EDTA), and then collected by centrifuging at 1500 r/min for 5 min, followed by re-suspension in phosphate-buffered saline (PBS). The cells were resuspended in 500 μL binding buffer with 5 μL Annexin V-FITC mix, and then 5 μL PI was added and mixed. This was followed by avoidance reaction at room temperature for 5–15 min and subsequent on-machine detection with flow cytometry.

### 2.3 Transmission electron microscopy

After transfection or treatment with miR-506 inhibitor and starvation for 12 h, cells were harvested and then fixed in a pH 7.4 buffer comprised of sodium cacodylate (0.1 mol/L), paraformaldehyde (2.0%, volume fraction), and glutaraldehyde (2.5%, volume fraction) at 4 °C for 12 h. The cells were then washed with buffer and fixed with osmium tetroxide (0.02 g/mL) at 25 °C for 1 h. Next, the samples were washed by buffer and distilled water (dH<sub>2</sub>O) in the appropriate order. The cell sediment was treated with gradient

ethanol dehydration series, and then infiltrated and embedded in the EMbed-812 (Electron Microscopy Sciences, 14900). Lead citrate was used to stain the sections of cells, and autophagy was observed under JEOL 1010 electron microscope (JEOL, Tokyo, Japan). A digital camera (Hamamatsu c4742-95, Hamamatsu, Japan) was used to capture the images of samples, which were analyzed by proprietary software.

#### 2.4 Construction of plasmids and dual-luciferase reporter experiment

The wild and mutated 3'-untranslated region (UTR) fragments of ETS1 were amplified and inserted into pGL3 luciferase reporter vector (Promega, Madison, WI, USA) within the restriction sites of *Xba*I. MiR-506 mimics (Sangon Biotech, Shanghai, China) combined with the pGL3 vector with the wild type or mutant 3'-UTR of ETS1 were co-transfected into U251 cells with Lipofectamine 3000 (Thermo Fisher Scientific, China) as per the instructions. After being transfected for 48 h, the luciferase activity of the cells was measured by a Renilla-Firefly Luciferase Dual Assay kit (Thermo Fisher Scientific).

The putative binding sites of the miR-506 promoter region with FOXO1 were predicted by the online system (<http://jaspar.genereg.net>). According to the foregoing prediction, the promoter regions of human miR-506 with different lengths were acquired by polymerase chain reaction (PCR) amplification from a template of genomic DNA extracted from U251 cells (primer sequences are shown in Table S1). Next, the fragments of amplification were separately interpolated into the regions between the sites of *Kpn*I and *Hind*III in the pGL3-basic vector (Promega), and the obtained plasmids were considered as follows. The region from -1800 to -1 bp of the fragment of the miR-506 promoter was designated as pGL3-F1, that from -1230 to -1 bp as pGL3-F2, and that from -500 to -1 bp as pGL3-F3. As for the assay of luciferase reporter, the plasmids obtained as above combined with pRL-TK vector expressing Renilla luciferase (Promega) were separately co-transfected with Lipofectamine 3000 (Invitrogen) into U251 cells based on the operation manual. After incubation for 12 h, the cells were collected, and luciferase activity was detected by the dual luciferase assay kit (Promega) according to the product manual. The firefly luciferase activity was normalized by Renilla luciferase activity.

#### 2.5 ChIP assay

Chromatin immunoprecipitation (ChIP) assays were performed by a ChIP assay kit (Merck-Millipore, USA) according to the manufacturer's instructions. The immunoprecipitation (IP) of chromatin DNA was performed with anti-FOXO1 antibody (CST, USA) or normal rabbit immunoglobulin G (IgG), followed by washing and cross-linking with DNA-protein-antibody. Quantitative PCR (qPCR) was performed to analyze the upstream of the miR-506 ATG initiation codon between -1800 and -1231 bp (p1), that between -1230 and -501 bp (p2), and that between -500 and -1 bp (p3 or F3), which were predicted including FOXO1-binding motifs in the promoter of miR-506. PCR amplification from -3146 to -2221 bp in the distal region was used as an NC. The primers for p1, p2, and p3 are listed in Table S1.

#### 2.6 In vivo tumor formation experiment

Forty female BALB/c nude mice were bought from Beijing Vital River Laboratory Animal Technology (Beijing, China) and bred in the specific pathogen free (SPF) grade animal house at our university. We injected  $2 \times 10^6$  U251 cells subcutaneously into the mice when they were aged 6–8 weeks and weighed around 18 g. After one week of inoculation, the mice were randomly divided into eight groups treated with FOXO1-OE or NC lentivirus (prepared according to our previous study (Chen et al., 2019)), miR-506 inhibitor, or ETS1 protein accompanied with TMZ (10 mg/kg i.g.) in 0.5% (5 g/L) carboxymethyl cellulose sodium (CMC-Na)/sterile water or an equal volume of solvent for two weeks. Then, all mice were allowed to be grown until sacrificed. The tumor diameters of the animals were measured every 2 or 3 d to calculate their volumes using the formula of  $\text{length}/2 \times \text{width}^2$ .

#### 2.7 Statistical analysis

Statistical analyses were performed by GraphPad Prism 9.4 (GraphPad Software Inc., USA). The data were shown as mean  $\pm$  standard deviation (SD). The differences between two groups were assessed by unpaired two-tailed Student's *t*-test. Comparisons between multiple groups were performed by one-way or two-way analysis of variance (ANOVA) with Dunnett's multiple comparisons test. A *P*-value of  $<0.05$  was considered as statistically significant.

More detailed information on materials and methods is shown in the supplementary information.

### 3 Results

#### 3.1 Interaction of miR-506 and FOXO1

We first explored the functions of FOXO1 and miR-506 in GBM. To identify the most suitable cell lines of GBM for further study, we detected miR-506-3p, miR-506-5p, and FOXO1 expression in various GBM cell lines. Both FOXO1 and miR-506 expression levels were downregulated in GBM cells of SHG-44, U251, U87, A172, and U373, compared with that in normal glia cells represented by HA (Figs. 1a–1c). The expression levels of miR-506-3p and FOXO1 in U251, and those of miR-506-5p and FOXO1 in A172 were lower than those in other GBM cells. Therefore, U251 and A172 were chosen for further study.

In order to explore the primary interaction of miR-506 and FOXO1, both U251 and A172 cells were transfected with FOXO1-OE plasmids (Fig. 1d), and the expression of miR-506 was evaluated by qPCR (Figs. 1e–1h). As shown in Fig. 1g, miR-506-3p was significantly higher expressed in U251 cells treated with FOXO1-OE ( $P < 0.05$ ). For the further investigation of FOXO1-miR-506 axis in GBM, miR-506-3p and U251 cells were chosen for subsequent study.

#### 3.2 Effects of FOXO1 and miR-506 on GBM chemosensitivity to TMZ

We next explored the effects of FOXO1 and miR-506-3p on GBM chemosensitivity to TMZ. The viability of U251 cells transfected with FOXO1-OE decreased significantly compared with that of cells transfected with NC plasmid under the same TMZ treatment condition (Fig. 2a). The inhibition of miR-506 attenuated the effect of FOXO1 on cell survival under exposure to TMZ (Fig. 2a). Consistent with the cell viability assay, FOXO1-OE-transfected cells under TMZ treatment showed poorer proliferation than other cells, and the miR-506 inhibitor practically enhanced cell proliferation (Figs. 2b and 2c). The result of the apoptosis assay indicated that FOXO1-OE under TMZ treatment tended to increase apoptosis in U251 cells compared with those only with TMZ treatment, while the miR-506 inhibitor induced less apoptosis to antagonize effect of FOXO1-OE (Figs. 2d–2g).

#### 3.3 Effects of FOXO1 and miR-506 on autophagy of GBM cells

Autophagy is a conserved recycling system that occurs under stress conditions, including chemotherapy, to maintain homeostasis through self-degradation (White and DiPaola, 2009; Cheng et al., 2018; Chun and Kim, 2018). Upregulated autophagy has a significant impact on chemoresistance in glioma cells (Simpson and Gammoh, 2020). Thus, we further evaluated the effects of FOXO1 and miR-506-3p on the autophagy of GBM cells. Transmission electron microscopy (TEM) images showed a decreased number of multiple double-membrane enclosed autophagosomes in U251 cells pre-transfected with FOXO1-OE compared with that in NC-transfected cells, and the miR-506 inhibitor tended to reverse the effect of FOXO1 (Fig. 3a). The expression of LC3 co-localized with lysosome-associated membrane glycoprotein 2 (LAMP2) decreased significantly in FOXO-OE cells compared with that in NC cells, and the miR-506 inhibitor also reversed the effect induced by FOXO1 (Fig. 3b).

Moreover, the expression of Beclin-1 and the relative protein expression of microtubule-associated protein 1A/1B-light chain 3 (LC3)-II/LC3-I decreased in FOXO1-OE transfected cells compared with the NC group, and miR-506 inhibitor could reverse the effect induced by FOXO1 (Figs. 3c–3e). All the above results indicated that overexpression of FOXO1 may inhibit autophagy in GBM cells through the regulation of miR-506.

#### 3.4 Effects of FOXO1 and miR-506 on the migration and invasion of GBM cells

High invasiveness is another determinant of local recurrence in GBM (Lim et al., 2020; Vollmann-Zwerenz et al., 2020). Transwell and scratch assays were conducted to investigate the invasion and migration of U251, respectively. Compared to U251 cells transfected with NC plasmids, cells transfected with FOXO1-OE plasmids were less invasive, which was attenuated by miR-506 inhibitor (Figs. 4a and 4b). Consistent with the invasion assay, FOXO1-OE plasmids transfected into U251 exhibited much lower migration ability, and miR-506 inhibitor increased their migration (Figs. 4c and 4d).

The EMT-related proteins E-cadherin and N-cadherin play critical roles in GBM (Xu et al., 2019;

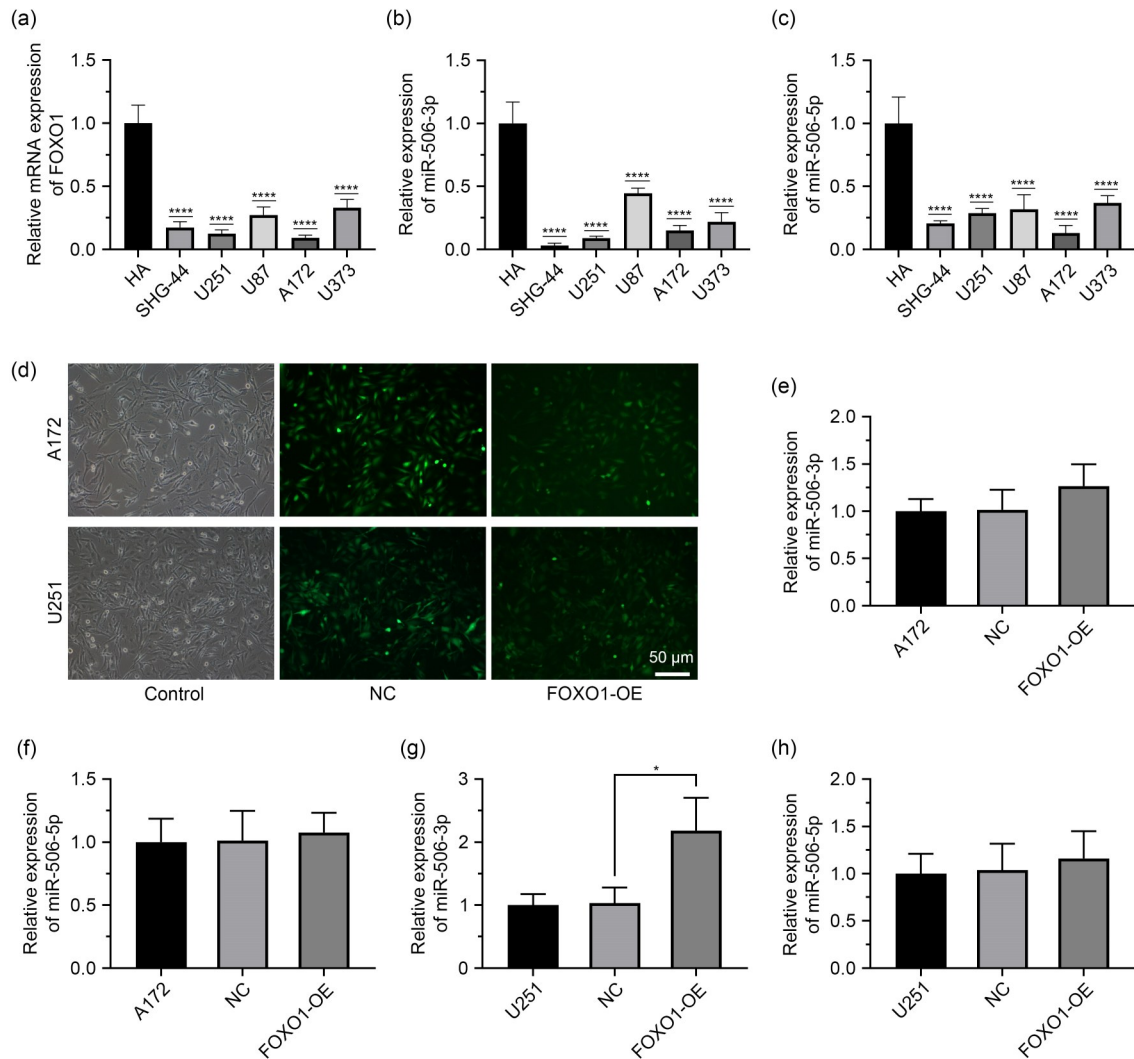


**Fig. 1** FOXO1 and miR-506 expression measured by qPCR in human normal glial cells (HA) and GBM cells (SHG-44, U251, U87, A172, and U373). (a) FOXO1 mRNA expression in glial and GBM cells. (b) MiR-506-3p expression in glial and GBM cells. (c) MiR-506-5p expression in glial and GBM cells. (d) A172 and U251 cells transfected with NC and FOXO1-OE plasmids. (e, f) MiR-506-3p and miR-506-5p expression in A172 cells transfected with NC/FOXO1-OE plasmids. (g, h) MiR-506-3p and miR-506-5p expression in U251 cells transfected with NC/FOXO1-OE plasmids. The data were expressed as mean $\pm$ SD,  $n=3$ . One-way ANOVA with Dunnett's multiple comparisons test: (a-c) \*\*\*\* $P<0.0001$  vs. HA; (g) \* $P<0.05$  vs. NC. ANOVA: analysis of variance; FOXO1: forkhead box protein O1; FOXO1-OE: FOXO1 overexpression; GBM: glioblastoma multiforme; HA: human astrocyte; mRNA: messenger RNA; NC: negative control; qPCR: quantitative polymerase chain reaction; SD: standard deviation.

Gao et al., 2021). N-cadherin upregulation can mediate adaptive radioresistance in GBM (Osuka et al., 2021). The western blotting results indicated that FOXO1 up-regulated E-cadherin expression significantly while it downregulated N-cadherin expression significantly in U251 cells, and miR-506 inhibitor could reverse the effect induced by FOXO1 (Figs. 4e and 4f). All the above data suggested that FOXO1-OE may inhibit GBM invasion through the regulation of miR-506.

### 3.5 Effect of FOXO1 on the expression of miR-506

From the bioinformatics analysis, we found that there were binding sites of FOXO1 in the miR-506 promoter (Fig. 5a). We constructed a series of luciferase reporter genes including different fragments of miR-506 promoter, which were then transfected into U251 cells separately. As shown in Fig. 5b, the pGL3-F1, F2, and F3 constructs showed significantly higher luciferase

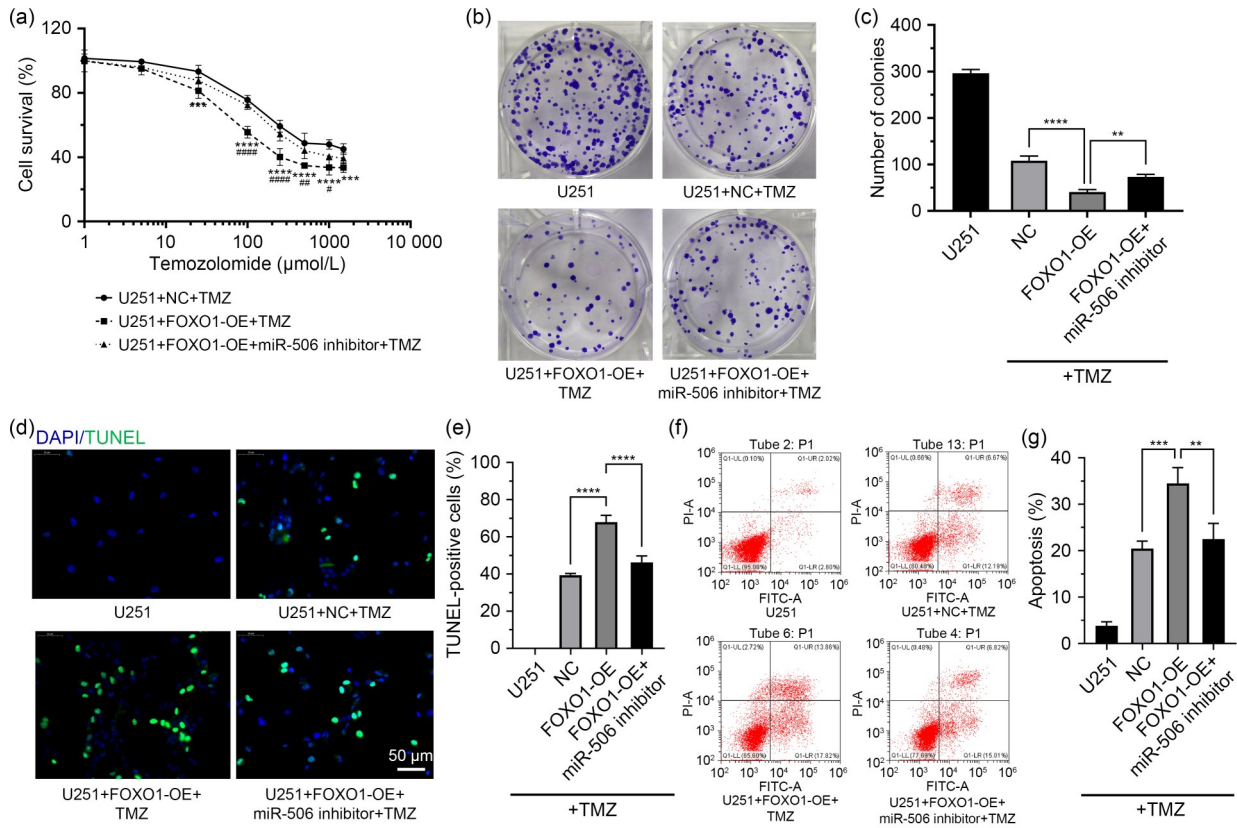


**Fig. 2** Effects of FOXO1 and miR-506 on GBM chemosensitivity to TMZ. U251 cells were transfected with FOXO1-OE or NC plasmids with/without miR-506-3p inhibitor accompanied with TMZ treatment. (a) The cell viability was assayed by CCK8 and the cell survival rate was analyzed. (b, c) Clone formation was evaluated and colony number was counted. (d, e) Cell apoptosis was measured using TUNEL staining, and TUNEL-positive cells were analyzed. (f, g) Cell apoptosis was evaluated using a flow cytometer. The data were expressed as mean±SD,  $n=3$ . (a) Two-way ANOVA with Dunnett's multiple comparisons test: \*\*\*  $P<0.001$ , \*\*\*\*  $P<0.0001$  vs. U251; #  $P<0.05$ , ##  $P<0.01$ , ####  $P<0.0001$  vs. U251+FOXO1-OE+miR-506 inhibitor. (e, g) One-way ANOVA with Dunnett's multiple comparisons test: \*\*  $P<0.01$ , \*\*\*  $P<0.001$ , \*\*\*\*  $P<0.0001$ . ANOVA: analysis of variance; CCK8: cell counting kit-8; FITC: fluorescein isothiocyanate; FOXO1: forkhead box protein O1; FOXO1-OE: FOXO1 overexpression; GBM: glioblastoma multiforme; NC: negative control; PI: propidium iodide; SD: standard deviation; TMZ: temozolomide; TUNEL: terminal deoxynucleotidyl transferase dUTP nick-end labeling.

activity when U251 cells were transfected with FOXO1-OE plasmids. Constructing pGL3 without miR-506 promoter fragments abolished the FOXO1-OE-induced luciferase activity. The results of ChIP assay indicated that the region of p3 (F3) was more immunoprecipitated with anti-FOXO1 than the other two regions in miR-506 promoter (Fig. 5c). These findings suggested that the region of p3 (F3) may harbor a major regulatory element. The result of electrophoretic mobility shift assay (EMSA) showed that 5'-TTTTGTATATTTTGTGTGTTTTT-3' (-311 to -288 bp) may be the main binding sites of FOXO1 and miR-506 promoter (Fig. 5d). All the above results indicated that FOXO1 upregulates miR-506 by binding to its promoter to enhance transcriptional activation.

### 3.6 Role of ETS1 in GBM growth by promoting FOXO1 translocation from the nucleus to the cytosol

MiR-506 has been demonstrated to inhibit EMT and angiogenesis in gastric cancer by targeting ETS1 (Li et al., 2015). From the bioinformatic analysis, we found that miR-506 may target the 3'-UTR of ETS1 (Fig. 5e). To explore the correlation between miR-506 and ETS1, we performed luciferase reporter assays. *ETS1* messenger RNA (mRNA) expression in the U251 cells transfected with miR-506-3p mimic decreased significantly compared with that in U251 cells transfected with the NC (Fig. 5f). The miR-506-3p mimic induced a significant luciferase activity decline in wild U251 cells, but there was no significant difference in luciferase activity with mutant 3'-UTR of ETS1 (Fig. 5g).

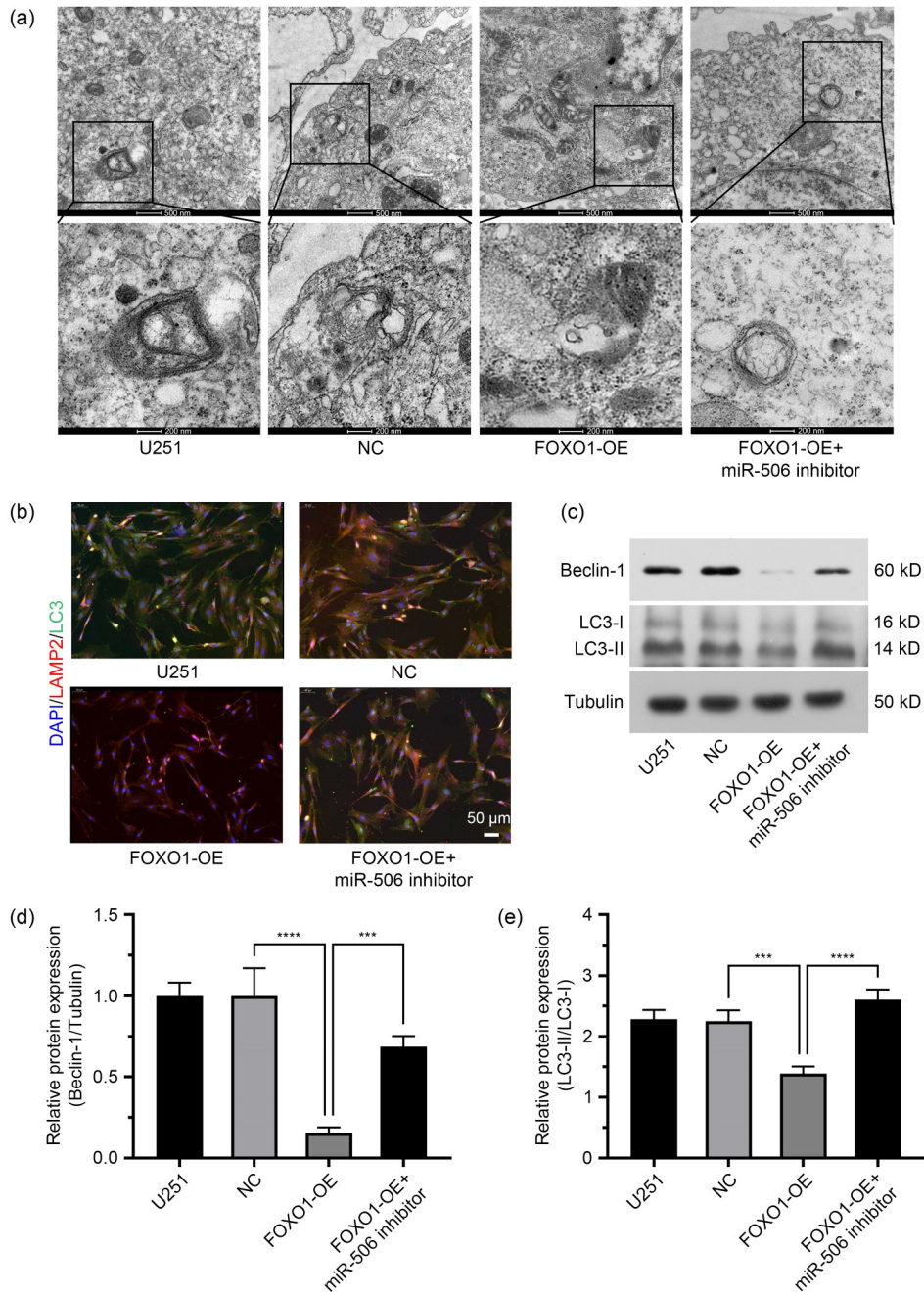


**Fig. 3** Effects of FOXO1 and miR-506 on autophagy in GBM. (a) Transmission electron microscopy images of U251 cells show multiple double-membrane-enclosed autophagosomes. A decreased number of autophagosomes were observed in cells transfected with FOXO1-OE compared with NC, and the miR-506 inhibitor could reverse this effect. Scale bar: 500 nm (upper) and 200 nm (lower). (b) Immunofluorescence assay of LC3 and LAMP2. There was lower LC3 expression accompanied with LAMP2 in FOXO1-OE cells compared with NC or normal U251 cells. The miR-506 inhibitor could reverse the effect induced by FOXO1-OE. Scale bar: 50  $\mu$ m. (c–e) The protein expression levels of Beclin-1 and LC3 were measured by western blotting. The data were expressed as mean $\pm$ SD,  $n=3$ . One-way ANOVA with Dunnett's multiple comparisons test: \*\*\*  $P < 0.001$ , \*\*\*\*  $P < 0.0001$ . ANOVA: analysis of variance; DAPI: 4',6-diamidino-2-phenylindole; FOXO1: forkhead box protein O1; FOXO1-OE: FOXO1 overexpression; GBM: glioblastoma multiforme; LAMP2: lysosome-associated membrane glycoprotein 2; LC3: microtubule-associated protein 1A/1B-light chain 3; NC: negative control; SD: standard deviation.

These results indicated that miR-506 may target the 3'-UTR of ETS1 to regulate ETS1 expression. Moreover,

ETS1 promotes FOXO1 protein exporting from the nucleus to inhibit the transcriptional activity of FOXO1.

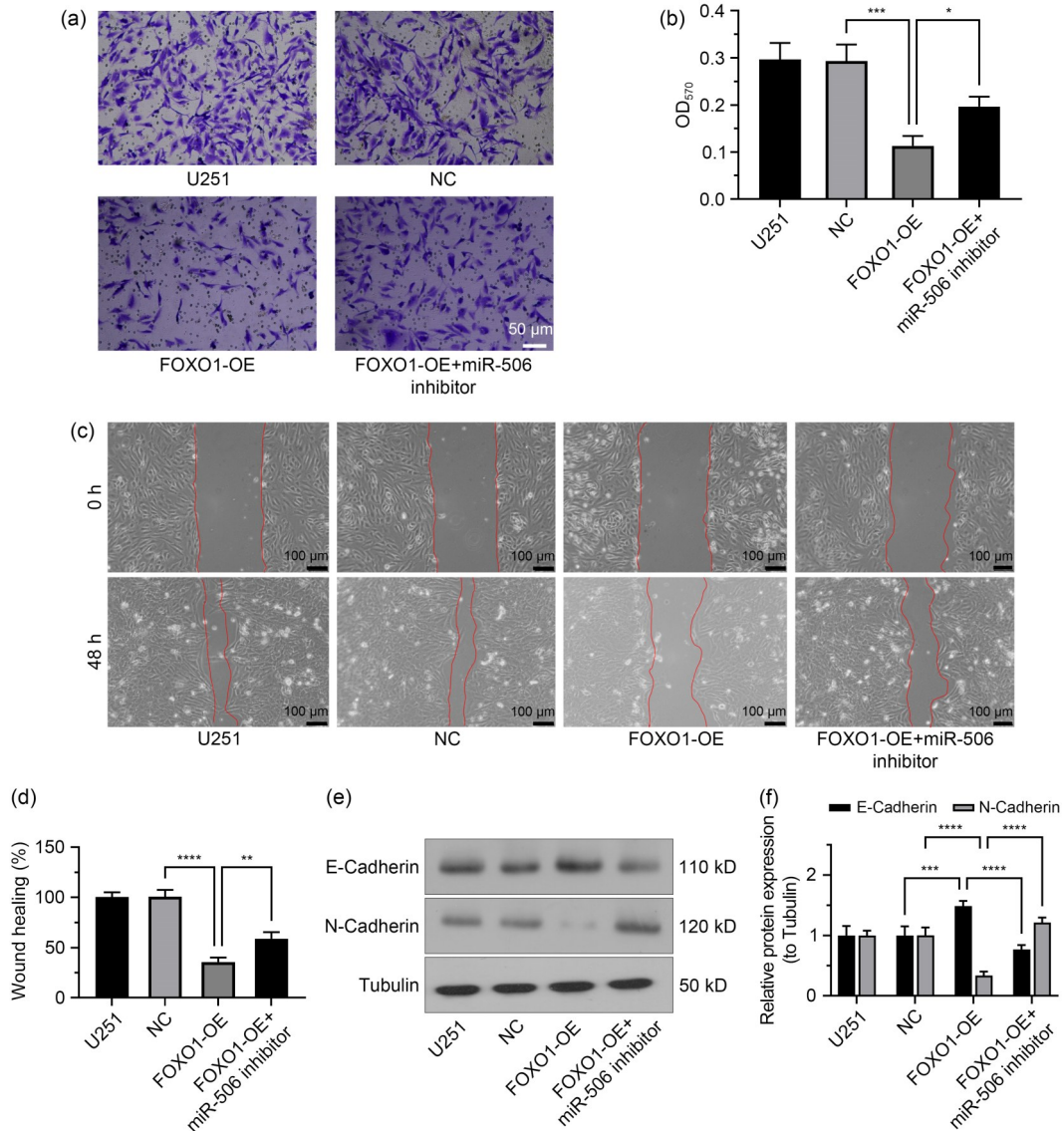


**Fig. 4** Effects of FOXO1 and miR-506 on the migration and invasion in GBM. U251 cells were transfected with FOXO1-OE or NC plasmids with/without miR-506-3p inhibitor. (a, b) Invasive ability of U251 measured using Transwell assay. (c, d) Migration ability of U251 measured using scratch assay. (e, f) Protein expression of E-cadherin and N-cadherin in U251 measured by western blotting. The data were expressed as mean±SD, *n*=3. One-way ANOVA with Dunnett's multiple comparisons test: \* *P*<0.05, \*\* *P*<0.01, \*\*\* *P*<0.001, \*\*\*\* *P*<0.0001. ANOVA: analysis of variance; FOXO1: forkhead box protein O1; FOXO1-OE: FOXO1 overexpression; GBM: glioblastoma multiforme; NC: negative control; OD<sub>570</sub>: optical density at 570 nm; SD: standard deviation.

As shown in Fig. 5h, the FOXO1 protein is mainly located in the nucleus of U251 cells, while ETS1-treated cells showed higher FOXO1 protein level in the cytoplasm.

### 3.7 Anti-tumor effect of TMZ enhanced by FOXO1 in GBM in vivo through a feedback loop of FOXO1/miR-506/ETS1/FOXO1

We further explored the role of FOXO1/miR-506/ETS1/FOXO1 loop in TMZ chemosensitivity in GBM

in vivo. As shown in Figs. 6a and 6b, the tumor volumes of mice treated with FOXO1-OE were significantly decreased compared with those of mice in the NC group. Both miR-506 inhibitor and ETS1 could reverse the effect of FOXO1-OE on tumor growth, which was similar to the corresponding test group with TMZ treatment (Figs. 6c and 6d). The result of Ki67 expression from immunohistochemistry assay showed that TMZ significantly inhibited Ki67 expression and FOXO1-OE strengthened the effect of TMZ. Moreover,



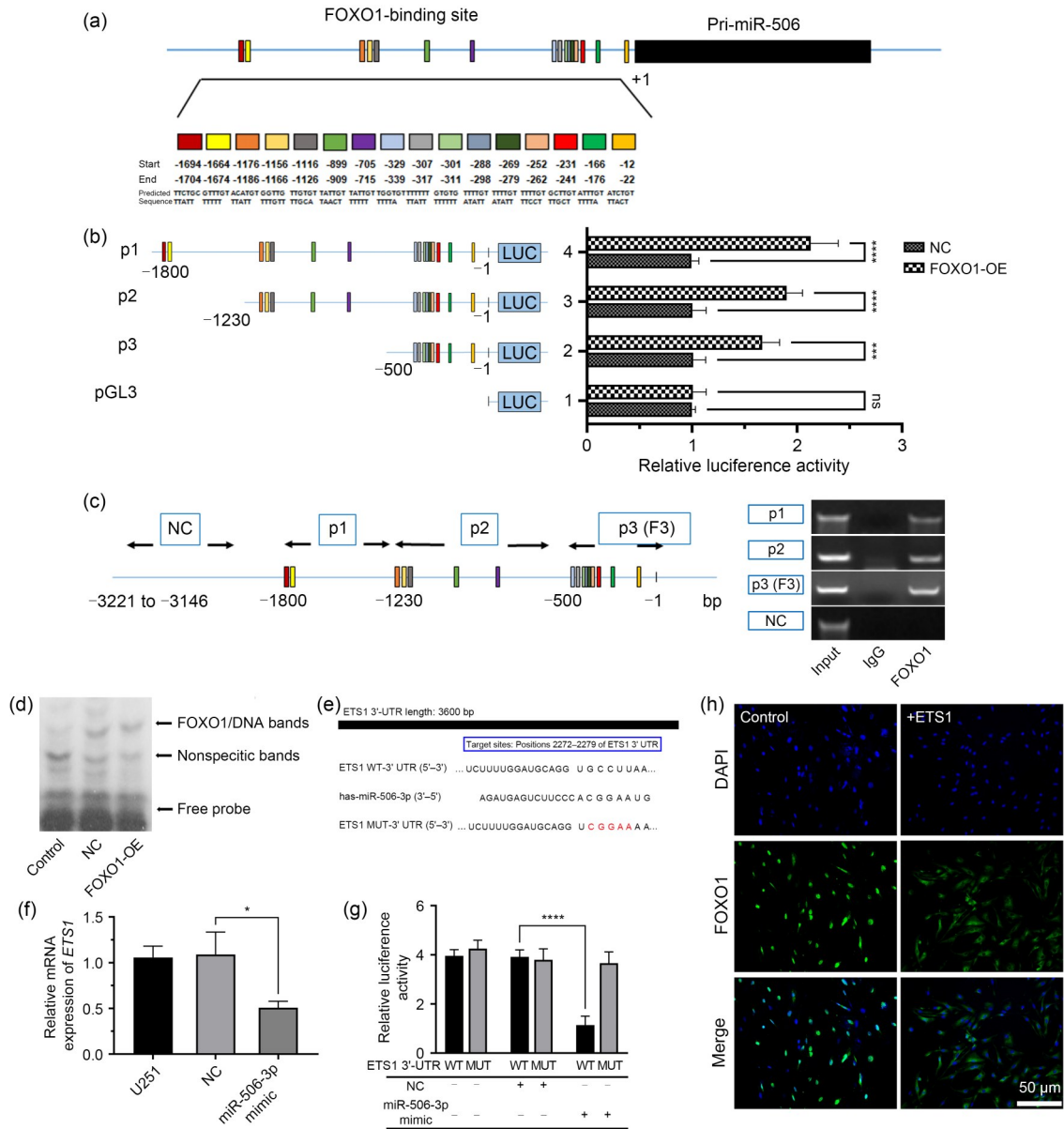


**Fig. 5** Negative feedback loop of FOXO1/miR-506/ETS1/FOXO1. (a) The putative FOXO1-binding sites in miR-506 promoter region were predicted using an online system (<http://jaspar.genereg.net>). (b) A series of luciferase reporters containing different fragments of miR-506 promoter region, such as (F1, pGL3 -1800 to -1 bp), (F2, pGL3 -1230 to -1 bp), (F3, pGL3 -500 to -1 bp), pGL3-basic, and FOXO1-OE or NC plasmids were transfected into U251 cells for luciferase assays. (c) Chromatin DNA was subjected to IP with anti-FOXO1 antibody or normal rabbit IgG. The recovered DNA was analyzed by qPCR for the presence of FOXO1-binding motifs at the miR-506 promoter between -1800 and -1231 bp (p1), between -1230 and -501 bp (p2), and between -500 and -1 bp (p3 or F3) upstream of the miR-506 ATG start codon. The distant region of -3221 to -3146 bp was used as an NC. (d) Electrophoretic mobility shift assay (EMSA) showed the binding sites of FOXO1 protein with miR-506 promoter. (e) Predicted binding site of miR-506-3p and 3'-UTR of ETS1 by TargetScan. (f) miR-506-3p mimic induced the downregulation of ETS1 measured by qPCR. (g) Dual luciferase reporter assays of miR-506-3p targeting 3'-UTR of ETS1 in U251 cells. (h) Immunofluorescence assay of FOXO1 protein in U251 cells with/without ETS1 treatment. The data were expressed as mean±SD,  $n=3$ . One-way ANOVA with Dunnett's multiple comparisons test: \* $P<0.05$ , \*\*\* $P<0.001$ , \*\*\*\* $P<0.0001$ ; ns: not significant. ANOVA: analysis of variance; DAPI: 4',6-diamidino-2-phenylindole; ETS1: E26 transformation-specific 1; FOXO1: forkhead box protein O1; FOXO1-OE: FOXO1 overexpression; IgG: immunoglobulin G; IP: immunoprecipitation; mRNA: messenger RNA; LUC: luciferase assay; MUT: mutant; NC: negative control; qPCR: quantitative polymerase chain reaction; SD: standard deviation; UTR: untranslated region; WT: wild type.

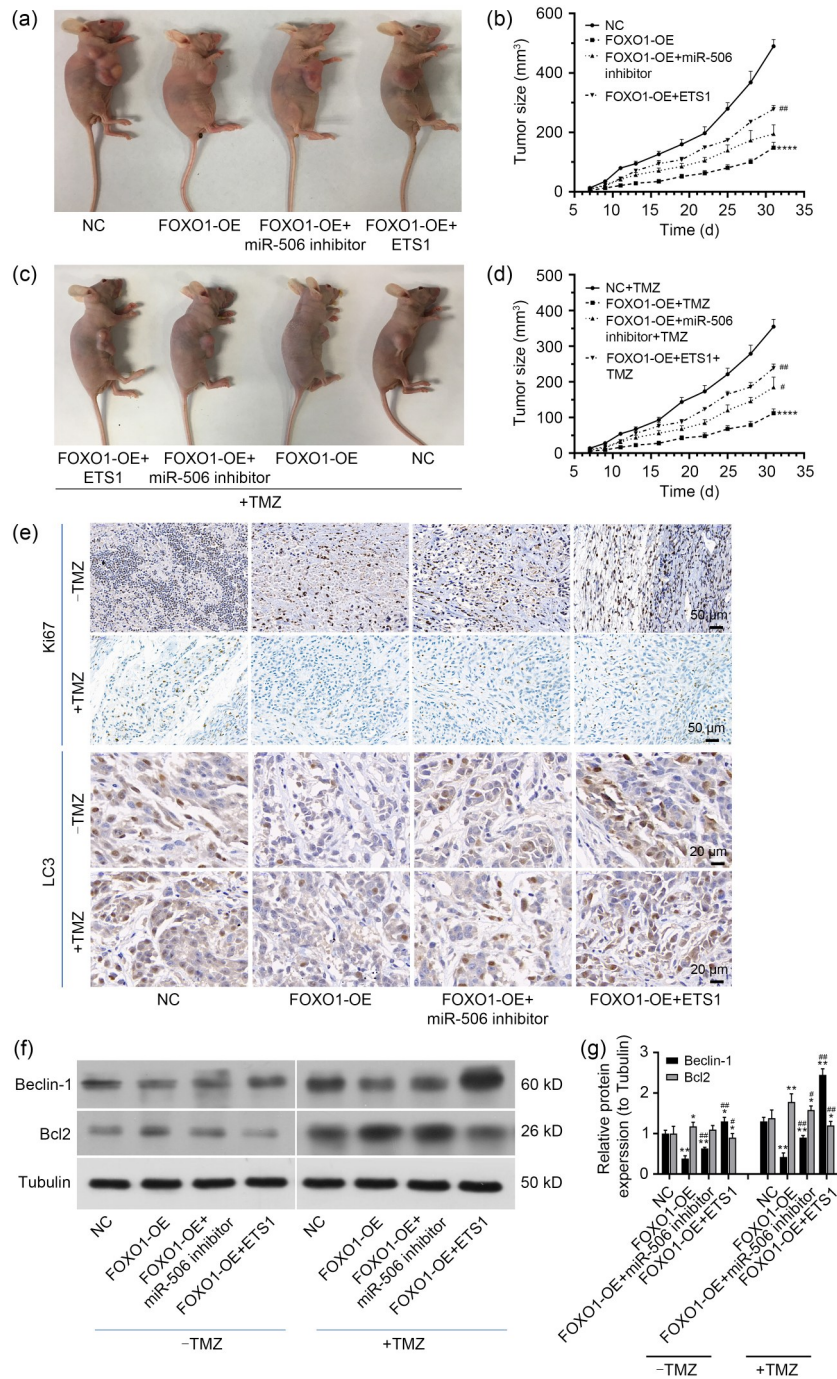


**Fig. 6** Anti-tumor effect of TMZ enhanced by FOXO1 in GBM through a feedback loop of FOXO1/miR-506/ETS1/FOXO1. Nude mice were subcutaneously injected with U251 and then intratumorally with FOXO1-OE virus, miR-506 inhibitor, or ETS1 protein accompanied with TMZ (10 mg/kg, i.g.) or an equal volume of solvent on Day 7 post-inoculation of tumor cells for two weeks. All animals were generally bred until sacrificed. (a, c) General images of tumor-bearing animals were taken at the end of experimental observation. (b, d) The length and width of tumors were measured to calculate tumor volume using  $\text{length}/2 \times \text{width}^2$ . (e) Immunohistochemistry staining was used to assay Ki67 and LC3. (f, g) The protein expression of Beclin-1 and Bcl2 was measured by western blotting. The data were expressed as mean  $\pm$  SD,  $n=5$ . One-way ANOVA with Dunnett's multiple comparisons test: \*  $P<0.05$ , \*\*  $P<0.01$ , \*\*\*\*  $P<0.0001$  vs. NC; #  $P<0.05$ , ##  $P<0.01$  vs. FOXO1-OE or FOXO1-OE+TMZ. ANOVA: analysis of variance; Bcl2: B-cell lymphoma-2; ETS1: E26 transformation-specific 1; FOXO1: forkhead box protein O1; FOXO1-OE: FOXO1 overexpression; GBM: glioblastoma multiforme; LC3: microtubule-associated protein 1A/1B-light chain 3; NC: negative control; TMZ: temozolomide; SD: standard deviation.

the miR-506 inhibitor or ETS1 attenuated the effect of FOXO1 on TMZ sensitivity (Fig. 6e). LC3 expression was measured by immunohistochemistry (Fig. 6e), and Beclin-1 expression was measured by western blotting (Figs. 6f and 6g). The data revealed that FOXO1-OE suppressed LC3 and Beclin-1 expression, and both miR-506 inhibitor and ETS1 could reverse the effect of FOXO1-OE. The result of western blotting for apoptosis-related protein B-cell lymphoma-2 (Bcl2) demonstrated that FOXO1-OE promoted Bcl2 expression, which was inhibited by both the miR-506 inhibitor and ETS1 (Figs. 6f and 6g). It is worth noting that TMZ enhanced the expression of LC3, Beclin-1, and Bcl2, which indicated that TMZ promoted autophagy and apoptosis.

#### 4 Discussion

As the most common malignant primary brain cancer in adults, GBM is notorious for its diffuse nature and resistance to radiotherapy and chemotherapy (Phillips et al., 2006; Paw et al., 2015). To the best of our knowledge, this study is the first to report that FOXO1-miR506 axis suppresses invasiveness and promotes chemosensitivity to TMZ in GBM through a feedback loop of FOXO1/miR-506/ETS1/FOXO1.

GBM has recently been classified into four different subtypes based on the gene expression patterns and clinical characteristics, including proneural, neural, classical, and mesenchymal (Verhaak et al., 2010; Zhao et al., 2021). GBM patients in the mesenchymal subgroup commonly have a worse prognosis due to the invasive spread of multiple lesions and much higher resistance to adjuvant radiotherapy and chemotherapy (Bhat et al., 2013). Similar to EMT, glial-mesenchymal transition (GMT) was reported to be associated with stem cell transformation, invasion, and resistance to chemoradiotherapy (Mahabir et al., 2014; Matias et al., 2017; Yachi et al., 2018). We found that the FOXO1-miR-506 axis inhibited GBM migration and invasion. The expression of the GMT-related marker E-cadherin decreased while that of N-cadherin increased, which indicated that the FOXO1-miR-506 axis could inhibit the mesenchymal transition of GBM.

FOXO1 is at a convergent point of RTK signaling (Jiang et al., 2018), which is one of the three core pathways implicated in GBM (The Cancer Genome

Atlas Research Network, 2008). Our previous study demonstrated that FOXO1 played a crucial role in GBM resistance to TMZ, carmustine (BCNU), and cisplatin (CDDP) (Chen et al., 2019). Here, we further clarified that FOXO1 promoted chemosensitivity via enhancing miR-506 promoter transcriptional activity to up-regulate the expression of miR-506. The binding site of FOXO1 on the miR-506 promoter was confirmed via online prediction and the dual luciferase reporter system. Moreover, miR-506-3p binds to the site of 3'-UTR of ETS1 that is involved in cell proliferation, survival, invasion, and angiogenesis, and is associated with poor prognosis and treatment resistance in cancers (Vishnoi et al., 2020). Further studies showed that ETS1 promotes exporting the FOXO1 protein out of nucleus. Therefore, FOXO1 enhances TMZ chemosensitivity in GBM through a feedback loop of FOXO1/miR-506/ETS1/FOXO1, which was confirmed both in vitro and in vivo.

As a highly conserved recycling system that occurs under stress conditions, autophagy is critical in maintaining cellular homeostasis by a series of proteins, in which cells maintain homeostasis through self-degradation. Autophagy has dual roles in tumor cell death and survival (White and DiPaola, 2009; Tomar et al., 2021; Fan et al., 2022). Although autophagy acts as a tumor suppressor, it is a mechanism of adaptation to stress response in tumor cells, helping in their survival during cancer therapy. Autophagy often leads to tumor resistance and refractory cancer by protecting cancer cells during chemotherapy. Upregulated autophagy has a significant impact on motility, cell survival, chemoresistance in glioma cells, and the maintenance of glioblastoma stem cells (GSCs) (Simpson and Gammoh, 2020). LC3 and Beclin-1 are the main markers of autophagy. Compared with the non-TMZ treatment group, the expression levels of LC3 and Beclin-1 were significantly upregulated in the TMZ treatment group, which indicated that autophagy could be involved in TMZ chemoresistance. FOXO1 could promote chemosensitivity to TMZ by inhibiting autophagy and downregulation of Beclin-1 levels and LC3-II/LC3-I expression, and the miR-506 inhibitor and ETS1 overexpression could reverse this effect. These results strongly indicated that FOXO1 could be a potential target to overcome TMZ chemoresistance in GBM.

However, there are limitations of this study: (1) the working mechanisms of ETS1 in the FOXO1/

miR-506/ETS1/FOXO1 loop and in the progression of GBM deserve further investigation; (2) besides the role of FOXO1-miR-506 axis that was confirmed in this study, the general gene map when overexpressing FOXO1 in GBM still needs to be explored. We aim to elucidate the above topics in our future work.

## 5 Conclusions

We have explored the role of a feedback loop of FOXO1/miR-506/ETS1/FOXO1 in GBM cell proliferation, apoptosis, migration, invasiveness, autophagy, and chemosensitivity to TMZ. Our results revealed that FOXO1 suppressed GBM cell invasiveness and promoted chemosensitivity to TMZ through enhancing miR-506 promoter transcriptional activity to up-regulate the expression of miR-506, which downregulated ETS1 expression by targeting its 3'-UTR, while ETS1 promoted exporting FOXO1 out of the nucleus to regulate its function. These findings provide evidence that the FOXO1/miR-506/ETS1/FOXO1 feedback loop might be a promising therapeutic target for GBM.

## Data availability statement

The datasets used and/or analyzed during the current study are available from the corresponding author upon reasonable request.

## Acknowledgments

This work was supported by the National Natural Science Foundation of China (Nos. 81402076, 81872072, and 82073274) and the Science Technology Commission of Shanghai Municipality (No. 20S11900700). We thank Dr. Yingmei LI (HaploX Biotechnology Co., Ltd., Shenzhen, China) for manuscript editing.

## Author contributions

Juxiang CHEN and Yufeng SHI conceived and designed the project. Chao CHEN and Yu'e LIU conducted experiments and drafted the manuscript. Hongxiang WANG performed data calculation and validation. Xu ZHANG collected samples and did all the bioinformatic work. All authors have read and approved the final manuscript, and therefore, have full access to all the data in the study and take responsibility for the integrity and security of the data.

## Compliance with ethics guidelines

Chao CHEN, Yu'e LIU, Hongxiang WANG, Xu ZHANG, Yufeng SHI, and Juxiang CHEN declared that they have no conflict of interest.

All institutional and national guidelines for the care and use of laboratory animals were followed. The animal experiments were carried out according to the guidelines of the Committee on Ethics of Medicine of Second Military Medical University (No. 20190122), Shanghai, China.

## References

- Bhat KPL, Balasubramanian V, Vaillant B, et al., 2013. Mesenchymal differentiation mediated by NF- $\kappa$ B promotes radiation resistance in glioblastoma. *Cancer Cell*, 24(3):331-346. <https://doi.org/10.1016/j.ccr.2013.08.001>
- Chen C, Xu T, Zhou JX, et al., 2013. High cytoplasmic FOXO1 and pFOXO1 expression in astrocytomas are associated with worse surgical outcome. *PLoS ONE*, 8(7): e69260. <https://doi.org/10.1371/journal.pone.0069260>
- Chen C, Han GS, Li YN, et al., 2019. FOXO1 associated with sensitivity to chemotherapy drugs and glial-mesenchymal transition in glioma. *J Cell Biochem*, 120(1):882-893. <https://doi.org/10.1002/jcb.27450>
- Cheng YC, Tsao MJ, Chiu CY, et al., 2018. Magnolol inhibits human glioblastoma cell migration by regulating N-cadherin. *J Neuropathol Exp Neurol*, 77(6):426-436. <https://doi.org/10.1093/jnen/nly021>
- Chun Y, Kim J, 2018. Autophagy: an essential degradation program for cellular homeostasis and life. *Cells*, 7(12):278. <https://doi.org/10.3390/cells7120278>
- de la Rosa J, Urdiciain A, Zazpe I, et al., 2020. The synergistic effect of DZ-NEP, panobinostat and temozolomide reduces clonogenicity and induces apoptosis in glioblastoma cells. *Int J Oncol*, 56(1):283-300. <https://doi.org/10.3892/ijo.2019.4905>
- Fan LX, Tao L, Lai YC, et al., 2022. Cx32 promotes autophagy and produces resistance to SN-induced apoptosis via activation of AMPK signalling in cervical cancer. *Int J Oncol*, 60:10. <https://doi.org/10.3892/ijo.2021.5300>
- Gao XY, Xia X, Li FY, et al., 2021. Circular RNA-encoded oncogenic E-cadherin variant promotes glioblastoma tumorigenicity through activation of EGFR-STAT3 signalling. *Nat Cell Biol*, 23(3):278-291. <https://doi.org/10.1038/s41556-021-00639-4>
- Jiang S, Li T, Yang Z, et al., 2018. Deciphering the roles of FOXO1 in human neoplasms. *Int J Cancer*, 143(7):1560-1568. <https://doi.org/10.1002/ijc.31338>
- Lapointe S, Perry A, Butowski NA, 2018. Primary brain tumours in adults. *Lancet*, 392(10145):432-446. [https://doi.org/10.1016/S0140-6736\(18\)30990-5](https://doi.org/10.1016/S0140-6736(18)30990-5)
- Li Z, Liu ZM, Dong SW, et al., 2015. MiR-506 inhibits epithelial-to-mesenchymal transition and angiogenesis in gastric cancer. *Am J Pathol*, 185(9):2412-2420. <https://doi.org/10.1016/j.ajpath.2015.05.017>
- Lim EJ, Kim S, Oh Y, et al., 2020. Crosstalk between GBM cells and mesenchymal stemlike cells promotes the invasiveness of GBM through the C5a/p38/ZEB1 axis. *Neuro Oncol*, 22(10):1452-1462. <https://doi.org/10.1093/neuonc/noaa064>

- Louis DN, Perry A, Wesseling P, et al., 2021. The 2021 WHO classification of tumors of the central nervous system: a summary. *Neuro Oncol*, 23(8):1231-1251.  
<https://doi.org/10.1093/neuonc/noab106>
- Lwin Z, MacFadden D, Al-Zahrani A, et al., 2013. Glioblastoma management in the temozolomide era: have we improved outcome? *J Neurooncol*, 115(2):303-310.  
<https://doi.org/10.1007/s11060-013-1230-3>
- Mahabir R, Tanino M, Elmansuri A, et al., 2014. Sustained elevation of Snail promotes glial-mesenchymal transition after irradiation in malignant glioma. *Neuro Oncol*, 16(5):671-685.  
<https://doi.org/10.1093/neuonc/not239>
- Matias D, Balça-Silva J, Dubois LG, et al., 2017. Dual treatment with shikonin and temozolomide reduces glioblastoma tumor growth, migration and glial-to-mesenchymal transition. *Cell Oncol (Dordr)*, 40(3):247-261.  
<https://doi.org/10.1007/s13402-017-0320-1>
- Osuka S, Zhu D, Zhang ZB, et al., 2021. N-cadherin upregulation mediates adaptive radioresistance in glioblastoma. *J Clin Invest*, 131(6):e136098.  
<https://doi.org/10.1172/JCI136098>
- Paw I, Carpenter RC, Watabe K, et al., 2015. Mechanisms regulating glioma invasion. *Cancer Lett*, 362(1):1-7.  
<https://doi.org/10.1016/j.canlet.2015.03.015>
- Phillips HS, Kharbanda S, Chen RH, et al., 2006. Molecular subclasses of high-grade glioma predict prognosis, delineate a pattern of disease progression, and resemble stages in neurogenesis. *Cancer Cell*, 9(3):157-173.  
<https://doi.org/10.1016/j.ccr.2006.02.019>
- Schneider B, Lamp N, Zimpfer A, et al., 2023. Comparing tumor microRNA profiles of patients with long- and short-term-surviving glioblastoma. *Mol Med Rep*, 27:8.  
<https://doi.org/10.3892/mmr.2022.12895>
- Simpson JE, Gammoh N, 2020. The impact of autophagy during the development and survival of glioblastoma. *Open Biol*, 10(9):200184.  
<https://doi.org/10.1098/rsob.200184>
- Singhal R, Bard JE, Nowak NJ, et al., 2013. FOXO1 regulates expression of a microRNA cluster on X chromosome. *Aging (Albany NY)*, 5(5):347-356.  
<https://doi.org/10.18632/aging.100558>
- The Cancer Genome Atlas Research Network, 2008. Comprehensive genomic characterization defines human glioblastoma genes and core pathways. *Nature*, 455(7216):1061-1068.  
<https://doi.org/10.1038/nature07385>
- Tomar MS, Kumar A, Srivastava C, et al., 2021. Elucidating the mechanisms of Temozolomide resistance in gliomas and the strategies to overcome the resistance. *Biochim Biophys Acta Rev Cancer*, 1876(2):188616.  
<https://doi.org/10.1016/j.bbcan.2021.188616>
- Verhaak RGW, Hoadley KA, Purdom E, et al., 2010. Integrated genomic analysis identifies clinically relevant subtypes of glioblastoma characterized by abnormalities in *PDGFRA*, *IDH1*, *EGFR*, and *NF1*. *Cancer Cell*, 17(1):98-110.  
<https://doi.org/10.1016/j.ccr.2009.12.020>
- Vishnoi K, Viswakarma N, Rana A, et al., 2020. Transcription factors in cancer development and therapy. *Cancers (Basel)*, 12(8):2296.  
<https://doi.org/10.3390/cancers12082296>
- Vollmann-Zwerenz A, Leidgens V, Feliciello G, et al., 2020. Tumor cell invasion in glioblastoma. *Int J Mol Sci*, 21(6):1932.  
<https://doi.org/10.3390/ijms21061932>
- Wang GJ, Jiao BP, Liu YJ, et al., 2019. Reactivation of microRNA-506 inhibits gastric carcinoma cell metastasis through ZEB2. *Aging (Albany NY)*, 11(6):1821-1831.  
<https://doi.org/10.18632/aging.101877>
- Wei C, Yang CG, Wang SY, et al., 2019. Crosstalk between cancer cells and tumor associated macrophages is required for mesenchymal circulating tumor cell-mediated colorectal cancer metastasis. *Mol Cancer*, 18:64.  
<https://doi.org/10.1186/s12943-019-0976-4>
- White E, DiPaola RS, 2009. The double-edged sword of autophagy modulation in cancer. *Clin Cancer Res*, 15(17):5308-5316.  
<https://doi.org/10.1158/1078-0432.CCR-07-5023>
- Xu B, Ma R, Russell L, et al., 2019. An oncolytic herpesvirus expressing E-cadherin improves survival in mouse models of glioblastoma. *Nat Biotechnol*, 37(1):45-54.  
<https://doi.org/10.1038/nbt.4302>
- Yachi K, Tsuda M, Kohsaka S, et al., 2018. miR-23a promotes invasion of glioblastoma via HOXD10-regulated glial-mesenchymal transition. *Signal Transduct Target Ther*, 3:33.  
<https://doi.org/10.1038/s41392-018-0033-6>
- Zhao Z, Zhang KN, Wang QW, et al., 2021. Chinese Glioma Genome Atlas (CGGA): a comprehensive resource with functional genomic data from Chinese glioma patients. *Genomics Proteomics Bioinformatics*, 19(1):1-12.  
<https://doi.org/10.1016/j.gpb.2020.10.005>

### Supplementary information

Materials and methods; Table S1